

FABRICATION OF LITHIUM-DOPED BIOLOGICAL-DERIVED HYDROXYAPATITE AND ZOLEDRONIC ACID BI-LAYERED STRUCTURES FOR IMPLANTOLOGY

OANA ANDREEA ZUREIGAT¹, JOHNY NEAMȚU¹, PAULA FLORIAN², MADALINA ICRIVERZI², LIVIA E. SIMA², ANDREI BIȚĂ¹, MARIA VIORICA CIOCÎLTEU¹, GABRIELA DORCIOMAN³, VALENTINA GRUMEZESCU³, GIANINA POPESCU-PELIN³, LIVIU DUTA^{3*}

¹Faculty of Pharmacy, University of Medicine and Pharmacy, 2 Petru Rareș Str., 200349 Craiova, Dolj County, Romania

²Institute of Biochemistry of the Romanian Academy, 296 Spl. Independenței, 060031 Bucharest, Romania

³Lasers Department, National Institute for Laser, Plasma and Radiation Physics, 409 Atomiștilor Str., 077125 Măgurele, Romania

*corresponding author: liviuduta@inflpr.ro

Manuscript received: November 2024

Abstract

In this study, lithium-doped biological-derived hydroxyapatite (BioHA:LiP) and BioHA:LiP functionalised with zoledronic acid (BioHA:LiP_ZA) structures were successfully fabricated using both pulsed laser deposition (PLD) and matrix-assisted pulsed laser evaporation (MAPLE) techniques. The structural, morphological, compositional, and biological properties of the deposited layers were investigated to evaluate their potential in implantology. X-ray diffraction and Fourier transform infrared spectroscopy confirmed the preservation of the HA phase and the successful incorporation of ZA into the coatings. Morphological assessments *via* scanning electron microscopy revealed compact granular morphologies characterised by tightly packed nanoscale particles forming a continuous film. At the same time, energy-dispersive X-ray spectroscopy validated the compositional integrity of the structures. Biological assays demonstrated the absence of cytotoxicity for all tested materials. Moreover, ZA doping was demonstrated to improve the adhesion and spreading of osteogenic progenitor stem cells. These findings suggest that ZA-functionalized BioHA:LiP coatings may exhibit promising characteristics for implant surface modifications and bone regeneration, supporting their further development for biomedical applications.

Rezumat

În acest studiu, au fost fabricate structuri de hidroxiapatită de origine biologică dopată cu litiu (BioHA:LiP) și funcționalizată cu acid zoledronic (BioHA:LiP_ZA) utilizând depunerea laser pulsată (PLD) și evaporarea laser pulsata asistata de o matrice (MAPLE). Proprietățile structurale, morfologice, compoziționale și biologice ale straturilor depuse au fost investigate pentru a evalua potențialul acestora în aplicațiile implantologice. Difracția de raze X și spectroscopia în infraroșu cu transformată Fourier au confirmat prezența HA și încorporarea cu succes a ZA în acoperiri. Evaluările morfologice realizate prin microscopie electronică de baleiaj au evidențiat morfologii granulare compacte, caracterizate prin particule nanometrice dispuse dens, formând un film continuu, în timp ce spectroscopia de raze X cu dispersie de energie a validat integritatea compozițională a structurilor. Testele biologice au demonstrat absența citotoxicității pentru toate materialele testate. În plus, s-a demonstrat că doparea cu ZA îmbunătățește adeziunea și răspândirea celulelor stem progenitoare osteogenice. Aceste rezultate sugerează că acoperirile BioHA:LiP funcționalizate cu ZA pot prezenta caracteristici promițătoare pentru modificarea suprafețelor implanturilor și regenerarea osoasă, susținând dezvoltarea lor ulterioară pentru aplicații biomedicale.

Keywords: bi-layered structures of lithium-doped biological-derived hydroxyapatite and zoledronic acid, cytocompatibility, metallic implants, pulsed laser deposition, matrix-assisted pulsed laser evaporation

Introduction

Implantable drug delivery systems have emerged as an innovative strategy for targeted therapy across various medical disciplines, particularly in treating bone-related diseases [1]. Among the most promising therapeutic agents utilised in these systems is zoledronic acid (ZA), a potent nitrogen-containing bisphosphonate. ZA is well-known for its capacity to inhibit bone resorption by osteoclasts, rendering it highly effective for conditions such as osteoporosis,

Paget's disease, bone metastases, and other skeletal complications associated with cancer [2].

Implantable systems designed for the delivery of ZA present several benefits over traditional administration methods, such as intravenous or oral routes [3, 4]. These systems enable a controlled, localised, and sustained drug release, which minimises systemic side effects and enhances therapeutic efficacy. By delivering ZA directly to the affected area - such as bone implants or prosthetics - these systems optimise drug concentration at the target site while mitigating potential

systemic toxicity, including renal complications and gastrointestinal side effects [5].

The materials employed in these implantable systems typically comprise biocompatible and biodegradable polymers (*e.g.*, polylactic-co-glycolic acid, PLGA), ceramics (*e.g.*, hydroxyapatite, HA), and metals (*e.g.*, titanium and its medical-grade alloys), which are commonly used in orthopaedic and dental implants [6]. Biological-derived HA (BioHA) is a carbonated, non-stoichiometric, calcium-deficient material characterised by reduced crystallinity. Consequently, it differs from synthetic HA in several key aspects, including composition, stoichiometry, crystal size and morphology, degree of crystallinity, degradation rate, and overall biological performance. Notably, studies have shown that HA derived from biowaste sources, such as eggshells, bovine bones, fish scales, and fish bones, can exhibit properties and behaviours that are comparable to, or even superior to, synthetic HA. This is attributed to the structural and compositional similarities between bone-derived apatites and naturally occurring apatites [7]. In addition to promoting optimal cell adhesion on the surface compared to the control (uncoated Ti), BioHA doped with lithium phosphate (BioHA:LiP) coatings have been shown to enhance the differentiation of human mesenchymal stem cells towards an osteoblastic phenotype [8]. These materials can be combined with ZA to serve a dual purpose: providing mechanical support while delivering therapeutic action. For instance, titanium implants coated with a ZA have demonstrated enhanced osseointegration (the bonding of bone to implant) and a reduced risk of implant failure due to their ability to inhibit osteoclast-mediated bone loss [9, 10].

Recent advancements in nanotechnology and surface engineering have further improved the efficiency of ZA delivery through implantable systems. Techniques such as plasma spray coating [11], electrospinning [12], and laser-assisted deposition [13] are employed to achieve precise drug loading and controlled release profiles. These innovations ensure that zoledronic acid retains its therapeutic effectiveness over extended periods, which is especially beneficial for patients requiring long-term bone stabilisation or regeneration. In this context, it is important to mention that the use of Pulsed Laser Deposition (PLD) and Matrix-Assisted Pulsed Laser Evaporation (MAPLE) to prepare bi-layered structures represents a novel and highly promising approach in the development of materials for biomedical applications. These advanced laser-based deposition techniques provide unparalleled precision and control over the fabrication of multi-layered structures with tailored properties, making them particularly suited for the demanding requirements of biomedical devices and implants. PLD, known for its ability to create thin films with precise stoichiometric transfer from target to substrate, allows for the deposition

of a wide range of materials, including metals, ceramics, and polymers. This versatility is crucial in biomedical applications, where compatibility with diverse substrates and controlled material properties, such as biocompatibility and biodegradability, are essential. MAPLE, on the other hand, offers a unique advantage in depositing organic and polymeric materials without compromising their molecular integrity, a common limitation of conventional thermal evaporation techniques. By using frozen solutions of the target material in a volatile solvent, MAPLE ensures the gentle transfer of sensitive biomolecules, making it ideal for applications requiring the integration of bioactive components. The combination of PLD and MAPLE to fabricate bi-layered structures is particularly innovative because it allows for the synergistic integration of different material properties within a single construct. For example, a PLD-deposited ceramic layer can provide mechanical strength and durability, while a MAPLE-deposited polymeric layer can offer bioactive or drug-eluting functionalities. This dual capability addresses a critical challenge in biomedical engineering: the need for multifunctional materials that meet mechanical, chemical, and biological requirements simultaneously.

Taking into consideration all these aspects, we report in the current work on the fabrication and characterisation of bi-layered structures made of BioHA:LiP and ZA coatings obtained by PLD and MAPLE techniques. It is worth emphasising that the ability to engineer multifunctional surfaces with controlled physical-chemical, mechanical and biological properties represent a significant advancement in the field. This approach opens new avenues for enhancing the efficacy of biomedical devices and lays the groundwork for innovative solutions in personalised medicine and tissue engineering.

Materials and Methods

Powder preparation

The BioHA powders were obtained from bovine femoral bones and purchased from a local market. Prior to use, the bones underwent veterinary inspection to ensure safety and compliance. The bones were cut into small pieces and thoroughly washed with distilled water. Subsequently, they were immersed in a 1% sodium hypochlorite solution for two weeks to facilitate deproteinisation.

After washing and drying, the bone pieces were calcined at 850°C for 4 h in the air using a Protherm oven (Alsarteknik Inc., Istanbul, Turkey).

The calcined bone pieces were then crushed by grinding, followed by processing in a ball mill to produce fine powders. A secondary calcination step was performed on the powders using the same protocol, with a controlled heating rate of 4°C/min.

The preparation process adhered to the standards of EU Regulation No. 722/2012 and ISO No. 22442-1:2015.

LiP powder (Sigma Aldrich, St. Louis, MI, USA) was incorporated into the BioHA powders at a concentration of 1 wt.%. Approximately 40 g batches of BioHA:LiP composite were prepared by mechanical mixing of the powders using a high-energy Retsch S 100 ball mill. The milling process was conducted in an open-air environment for approximately 15 min. at a rotational speed of 200 RPM.

Targets preparation

Approximately 2.5 g of BioHA:LiP powder mixtures were introduced into a stainless-steel mould (Specac Ltd., Orpington, UK) with a diameter of 2 cm. The powder mixtures were then compacted by applying a pressure of ~6 MPa, resulting in the formation of pellets with an approximate thickness of 0.5 cm. These pellets were subsequently sintered at 700 °C for 4 h, with a controlled heating rate of 5°C/min, followed by natural cooling. The sintered pellets were then utilised as targets for pulsed laser deposition (PLD) experiments.

ZA powder (Sigma Aldrich, St. Louis, MI, USA) was suspended in 10 mL of deionised water. The solution was prepared in an Erlenmeyer flask under continuous stirring. Approximately 4 mL of the prepared solution was transferred into a copper cup (30 mm in diameter and 5 mm in height), frozen at liquid nitrogen temperature (77 K), and subsequently employed as a target for matrix-assisted pulsed laser evaporation (MAPLE) experiments.

Synthesis of bi-layered structures

All experiments were conducted in a stainless-steel deposition chamber using a pulsed UV KrF* COMPexPro 205F excimer laser ($\lambda = 248$ nm, $\tau_{\text{FWHM}} \leq 25$ ns) (Coherent, Santa Clara, CA, USA), operated at a repetition rate of 10 Hz for PLD and 13 Hz for MAPLE. The depositions followed a two-step procedure: first, one set of samples (BioHA and BioHA:LiP) was synthesised using the PLD technique. Subsequently, a second set was fabricated *via* the MAPLE method by depositing ZA (1 wt.%) onto the PLD thin films, forming BioHA:LiP-ZA bi-layered structures.

The ablated material was transferred and deposited onto medical-grade Ti substrates ($\phi = 12$ mm, thickness = 1.5 mm) and double-side polished Si (100) wafers ($\sim 1 \times 1$ cm²) (Medapteh Plus Cert SRL, Măgurele, Romania). The substrates were positioned parallel to the target surface at a separation distance of ~5 cm. Before being placed in the deposition chamber, all substrates were cleaned in an ultrasonic bath (Elmasonic X-tra 30H, Elma Schmidbauer GmbH, Singen, Germany).

The laser beam was incident at a 45° angle to the target surface, with the fluence set to 4 J/cm² for PLD and 300 mJ/cm² for MAPLE. To ensure a uniform laser spot and reproducibility of the samples, a

dedicated single-axis beam homogeniser was used in all MAPLE experiments.

During PLD depositions, all substrates were heated and maintained at a constant temperature of 500°C using a PID-Excel temperature controller (Excel Instruments, Mumbai, India). The heating and cooling rates were set to 20 °C/min and 10 °C/min, respectively. In contrast, all MAPLE experiments were conducted at room temperature (RT).

To prevent piercing and potential surface morphology modifications caused by laser radiation, both PLD and MAPLE targets were continuously rotated during the multi-pulse deposition process at a frequency of 0.83 Hz (50 rotations *per* minute). For the fabrication of each coating, 15,000 laser pulses for PLD and 100,000 pulses for MAPLE were applied.

The PLD experiments were conducted in water vapour-enriched ambient at a residual pressure of $\sim 5 \times 10^{-1}$ mbar, whereas MAPLE depositions were performed at a pressure of $\sim 2.3 \times 10^{-4}$ bar.

The as-deposited PLD coatings underwent post-deposition thermal treatments at 500°C, the same temperature used during deposition, in a water vapour-enriched ambient for 6 h.

Chemicals and reagents used for sample preparation in chromatographic measurements

Chemicals and reagents

High-performance thin-layer chromatography (HPTLC) plates coated with silica gel 60 F254 were obtained from Merck. The mobile phase was prepared by dissolving di-potassium hydrogen phosphate anhydrous (400 mg) and tetra-n-butylammonium hydrogen sulphate (TBAHS, 200 mg) in 100 mL of a water-methanol mixture in a 9:1 (v/v) ratio [14]. All reagents utilised in the preparation were of analytical grade.

Sample preparation

A stock solution of ZA was prepared by dissolving 10 mg of the compound in 10 mL of deionised water, resulting in a concentration of 1 mg/mL. Serial dilutions were subsequently performed to prepare working solutions with concentrations ranging from 10 µg/mL to 50 µg/mL.

Chromatographic conditions

The HPTLC analysis was conducted using silica gel 60 F₂₅₄ plates. Standards were applied to the plates as 5 µL bands, while samples were applied as 10 µL bands using a CAMAG Linomat 5 applicator. The bands were spaced 11.4 mm apart and positioned 8 mm from the bottom edge of the plate. Elution was performed over a distance of 40 mm from the bottom edge of the plate in a pre-saturated twin-trough chamber.

Characterization methods of the synthesised bi-layered structures

The chemical structure of the fabricated structures was analysed using Fourier transform infrared (FTIR) spectroscopy. The measurements were conducted with an IRTracer-100 spectrometer

(Shimadzu), operating in attenuated total reflectance (ATR) mode and equipped with a diamond ATR crystal (0.18 cm diameter). All spectra were acquired at room temperature (RT) over the wavenumber range of 3000 - 500 cm^{-1} , with a resolution of 4 cm^{-1} , and averaged from a total of 64 scans *per* experiment. *X-ray diffraction* investigations were conducted using a Panalytical X'Pert Pro MPD system (PANalytical, NL) with $\text{CuK}\alpha$ radiation ($\lambda = 1.5418 \text{ \AA}$). The diffraction patterns were recorded in symmetric geometry (Bragg-Brentano) over an angular range of (10 - 90) $^\circ$ (2θ), with a step size of 0.02 $^\circ$ and an acquisition time of 15 seconds *per* step. *The surface morphology* of the fabricated structures was analysed using an Apreo S SEM microscope (ThermoFisher Scientific, Waltham, MA, USA),

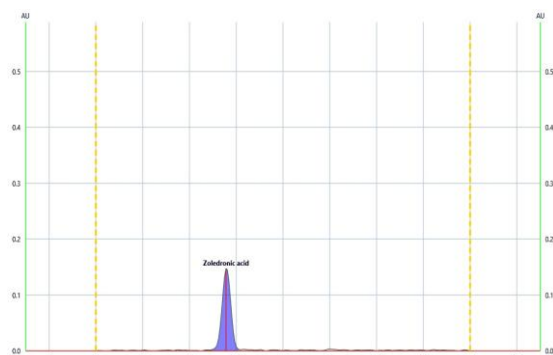


Figure 1.

A densitogram of zoledronic acid showing a distinct peak at an Rf value of 0.38 was detected at a wavelength of 215 nm

In vitro cell assays

Cell culture

Human mesenchymal stem cells (hMSCs), obtained as previously described [15, 16], were grown in Dulbecco's Minimal Essential Medium GlutaMAX[®] with low glucose content (1 g/L), supplemented with 10% (v/v) heat-inactivated fetal bovine serum (FBS) and 1% penicillin-streptomycin (PE/ST). Cells were maintained in a humidified atmosphere at 37 $^\circ\text{C}$ with 5% CO_2 . All experiments were conducted using hMSCs at passages 14 - 16, with viability exceeding 95%, as assessed by 0.4% Trypan Blue reagent. Prior to *in vitro* experiments, all tested materials were sterilised using UV radiation for 15 min in a Thermo Safe hood.

Cell Viability Assay

To evaluate the effect of surface materials on hMSC viability, cells were seeded at a density of 5000 cells/ cm^2 in 24-well plates and allowed to grow for 72 h in a humidified atmosphere at 37 $^\circ\text{C}$ with 5% CO_2 . A colorimetric cell viability assay (CellTiter 96[®] Aqueous One Solution Proliferation Assay kit, Promega) was employed to assess the viability of

operated under a high vacuum in secondary electron mode, with an acceleration voltage of 10 kV.

The SEM investigations were supplemented with energy-dispersive X-ray spectroscopy (EDS) to determine the chemical composition of the thin films. The analyses were performed using an EDAX Octane Elite EDS/EDX system operated at an acceleration of 10 kV. To ensure experimental reproducibility, EDS analyses were conducted in four randomly selected areas of the deposited films on the sample surfaces. Following elution, the HPTLC plates were dried for 10 minutes using a cold air stream provided by an air dryer. Detection and quantification were carried out at a wavelength of 215 nm using a CAMAG Scanner 3. The plates were scanned, and the resulting data were analysed with VisionCATS software (version 3.2 SP2) by CAMAG.

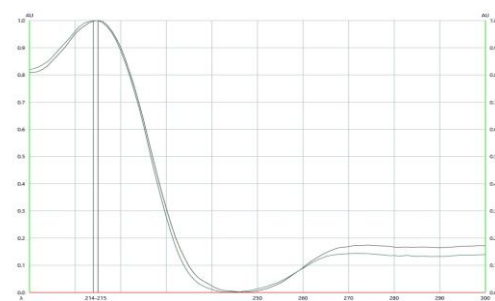


Figure 2.

UV spectra comparison of zoledronic acid reference standard (grey curve) and sample (green curve) showing consistent absorbance profiles, with maximum absorbance observed at 214 nm for the sample and 215 nm for the reference, respectively

cells in direct contact with the surface. Briefly, materials with adherent living cells were carefully transferred to a new plate and incubated for 2 h with MTS tetrazolium reagent (1:5 dilution in complete medium) at 37 $^\circ\text{C}$, protected from light. Following incubation, 100 μL of the formazan product was collected and transferred to a clear-bottom 96-well plate. The optical density at 450 nm was measured using a microplate reader (Mithras Berthold LB 940, Berthold Technologies, Bad Wildbad, Germany), with absorbance values directly proportional to the viable cell density on the surface material.

In addition to the direct contact evaluation, an indirect contact assessment was performed. Specifically, hMSCs adhered to the 24-well culture plate were exposed to the conditioned medium obtained from modified and unmodified Ti surfaces, which had been immersed for 72 h.

Fluorescence assay of cytoskeleton and cell adhesion

A density of 5000 cells/ cm^2 was seeded and cultured for 72 h in direct contact with the surface materials. Following fixation with 4% paraformaldehyde for

20 min, cells were permeabilised with 0.2% Triton X-100 for 3 min at room temperature. To minimise non-specific binding, cells were blocked for 1 h with 0.5% bovine serum albumin (BSA) in PBS. Actin filaments were then stained by incubating the samples for 30 min with Alexa Fluor 488-conjugated phalloidin (Invitrogen A12379, Life Technologies) diluted 1:100 in 0.5% BSA-PBS. Cell nuclei were counterstained with Hoechst (1 $\mu\text{g}/\text{mL}$, H-21492 Life Technologies, Molecular Probes, Eugene, OR, USA), and samples were subsequently mounted with FluoroSave reagent (#345789, Millipore).

Fluorescence images were acquired using a Zeiss AxioCam ERc5s Apotom 2 microscope equipped with an EC Plan-Neofluar 10 \times objective. Image analysis was performed using AxioVision Rel. 4.8 software (Zeiss).

Statistical analysis

Statistical analysis of cell viability data was conducted using GraphPad Prism 6 software (GraphPad, San Diego, CA, USA). One-way ANOVA followed by Tukey's multiple comparison test was applied to assess statistical differences. All biological assays were performed in triplicate. Data are expressed as mean \pm standard deviation (SD), with p values < 0.05 considered statistically significant.

Results and Discussion

HA-based coatings have been extensively investigated for their potential in biomedical applications, particularly

in bone tissue engineering and implantology. The incorporation of bioactive ions and pharmaceutical agents into HA structures has been explored as a strategy to enhance their biological performance, improve osteointegration, and impart specific therapeutic functionalities. The present study aims to evaluate the structural, morphological, compositional, and biological properties of HA-based thin films functionalised with ZA. The following sections present and discuss the obtained results, highlighting the implications of ZA incorporation.

FTIR

Figure 3 illustrates comparative FTIR spectra of BHA:LiP thin film (black line) and BHA:LiP_ZA bi-layered structures (red line). Significant structural and compositional differences between the two types of structures were revealed. Thus, the spectrum of the BHA:LiP sample exhibits characteristic vibrational modes of HA, with notable peaks around 560 cm^{-1} and 600 cm^{-1} , corresponding to the O–P–O bending vibrations of phosphate (PO_4^{3-}) groups. Additionally, the symmetric (near 960 cm^{-1}) and asymmetric (1040 and 1100 cm^{-1}) stretching vibration modes of PO_4^{3-} appear prominently, confirming the presence of a crystalline HA structure.

The characteristic OH^- stretching mode of HA appears as a weak librational mode around $\sim 630\text{ cm}^{-1}$, and is usually associated with the presence of hydroxyl groups in HA and their interaction with other functional groups.

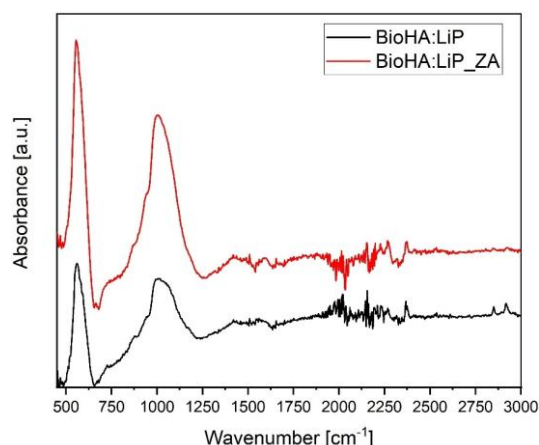


Figure 3.

FTIR spectra of biological hydroxyapatite doped with lithium phosphate (BioHA:LiP, black line) thin film and bi-layered structures of BioHA:LiP and Zoledronic acid (BioHA:LiP_ZA, red line)

Upon the deposition of ZA (BHA:LiP_ZA sample), significant spectral changes are observed. The most striking feature is the increased intensity and sharpness of the phosphate-related peaks, particularly in the regions of $560\text{--}600\text{ cm}^{-1}$ and $1000\text{--}1100\text{ cm}^{-1}$, indicating an enhancement in structural order and potential modifications in crystallinity. The sharper peaks suggest the improved organisation of the HA

lattice, likely influenced by the interaction of ZA with the phosphate groups. Moreover, bands in the region of $750\text{--}900\text{ cm}^{-1}$ are more defined and intense now, which can be related to the stretching vibrations of the P–O bonds in ZA, confirming its successful incorporation into the thin film and a possible structural stabilisation.

One should note that a weak band observed around $\sim 1200\text{ cm}^{-1}$ is characteristic of phosphonate groups in ZA, while peaks in the region of $\sim 1400\text{--}1500\text{ cm}^{-1}$ can be attributed to C=N and C–N stretching vibrations from the imidazole moiety. Additionally, the overall spectral baseline in the $1500\text{--}2500\text{ cm}^{-1}$ range appears noisier in the BHA:LiP_ZA sample, which may be attributed to organic components from the ZA molecule. The subtle variations in this range may also indicate hydrogen bonding interactions between ZA and the HA matrix. The presence of distinct spectral features in BHA:LiP_ZA confirms that the deposition of ZA by MAPLE has successfully altered the surface chemistry of the thin film, potentially enhancing its overall biocompatibility.

XRD

The XRD patterns corresponding to the BioHA:LiP coatings (black line) and the BioHA:LiP_ZA bi-layered structures (red line) are comparatively presented in Figure 4. The XRD analysis confirmed that the investigated samples predominantly consist of an HA-like compound, as referenced in ICDD: 00-009-0432. The most intense peaks in the patterns presented in Figure 4 correspond to the Ti substrate (ICDD: 44-1294). Consequently, the intensity scales of the graphical representations were adjusted to highlight the lower-intensity diffraction lines originating from the deposited films/structures.

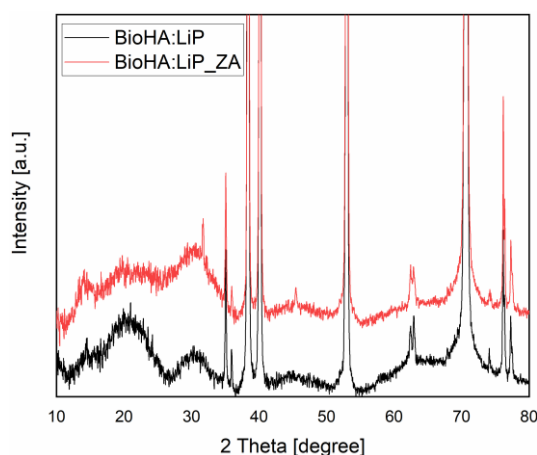


Figure 4.

Comparison of the X-ray diffractograms recorded for the biological hydroxyapatite doped with lithium phosphate (BioHA:LiP, black line) thin film and bi-layered structures consisting of BioHA:LiP and Zoledronic acid (BioHA:LiP_ZA, red line)

The diffractogram corresponding to the BioHA:LiP film (black line in Figure 4) exhibits characteristic peaks associated with HA at $2\theta \approx 25.9^\circ$ (002), 31.8° (211), 32.2° (112), 39.8° (310), 46.7° (222), 49.5° (213), 53.2° (004), 64.0° (323), and 77.0° (004). In contrast, the diffractogram of the BioHA:LiP_ZA structure displays similar peaks but with notable differences. Specifically, an increase in background intensity between 10° and 30° is observed, which may be attributed to the presence of an additional phase, likely related to the ZA deposition. Furthermore, the relative intensities of certain HA peaks, particularly those around $31\text{--}33^\circ$ and 45° , appear enhanced in BioHA:LiP_ZA, suggesting a possible structural modification due to the interaction between ZA and HA. Overall, it can be observed that the peaks in the BioHA:LiP_ZA structures exhibit increased sharpness and intensity compared to those in the BioHA:LiP coatings. This suggests (i) a higher degree of crystallinity in BioHA:LiP_ZA and (ii) the presence of additional reflections, likely associated with ZA, which may enhance or modify the HA structure. Notably, this result aligns with the FTIR findings.

SEM

The surface morphologies of the fabricated thin films (BioHA:LiP and BioHA:LiP_ZA) and drop-cast (ZA_DC) are presented comparatively in Figure 5. SEM investigations were conducted at $25,000\times$ magnification to highlight the microstructural details. BioHA:LiP (Figure 5, left image) shows a compact granular morphology characterised by tightly packed nanoscale particles forming a continuous film. The uniform distribution of granules suggests a successful deposition process with minimal agglomeration. This structure is indicative of the crystalline nature of BioHA, modified by LiP doping. ZA_DC (Figure 5, centre image) exhibits a starkly different morphology, with discrete, isolated spherical particles of varying sizes. The absence of a continuous matrix indicates that drop-casting results in non-uniform deposition, which could be attributed to the drying dynamics of the ZA solution. This morphology may lead to a heterogeneous distribution of functional properties across the surface. In contrast, BioHA:LiP_ZA (Figure 5, right image) displays a hybrid structure, where the granular morphology of

the BioHA:LiP base film is still apparent, but larger particles, likely of ZA, are dispersed on the surface. These larger structures provide a dual-scale morphology, with nanoscale granules and microscale ZA features,

which is advantageous for enhancing surface functionality (*e.g.*, drug loading and release or improved cell-surface interactions).

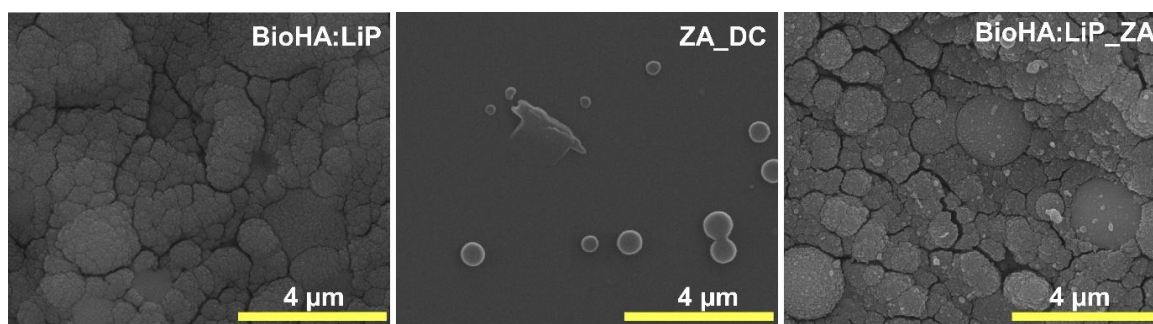


Figure 5.

Top-view SEM micrographs of BHA:LiP film, BHA:LiP_ZA bi-layered structure, and ZA dropcast (ZA_DC). Magnification bars: 4 µm

EDS

Besides the characteristic constituents of HA, namely Ca, P, and O, the compositional analysis identified trace amounts of additional elements, such as Na, Mg, and Si. Apart from the aforementioned elements naturally found in the chemical composition of healthy bone tissue, no other impurity species were detected within the sensitivity limits of the employed analytical technique.

EDS investigations indicated that the Ca/P atomic ratios for the BioHA:LiP and BioHA:LiP_ZA structures were 1.45 ± 0.01 and 1.49 ± 0.01 , respectively. These values are consistent with those reported for HA of biological origin [17, 18]. It is important to note that the observed shift in the Ca/P ratio toward a slightly higher value in BioHA:LiP_ZA structures, compared to BioHA:LiP films, indicates successful ZA adsorption. This effect can be attributed to ZA interactions with phosphate sites on HA, leading to the partial replacement or masking of some PO_4^{3-} groups. Furthermore, ZA deposition also influences

the P signal intensity, which increases from 6.79 ± 0.7 (BioHA:LiP) to 8.04 ± 0.1 (BioHA:LiP_ZA). This increase suggests the presence of additional phosphonate groups from ZA within the BioHA:LiP_ZA synthesised structures.

HPTLC

The data presented in Figure 6 indicates the release profile of ZA from Ti-BioHA-ZA structures over a period of 72 h. The release of ZA remains relatively stable during the first 24 hours, showing only a slight decrease from $11.75 \mu\text{g/mL}$ to $11.66 \mu\text{g/mL}$. This suggests a controlled and sustained release during the initial phase, possibly due to the diffusion from the BioHA coating. After 24 h, a significant drop in the release concentration is observed, with values decreasing to $8.653 \mu\text{g/mL}$ at 48 h and further to $7.619 \mu\text{g/mL}$ at 72 h. This decline could indicate the depletion of surface-adsorbed ZA and a transition toward slower diffusion from deeper layers within the BioHA matrix.

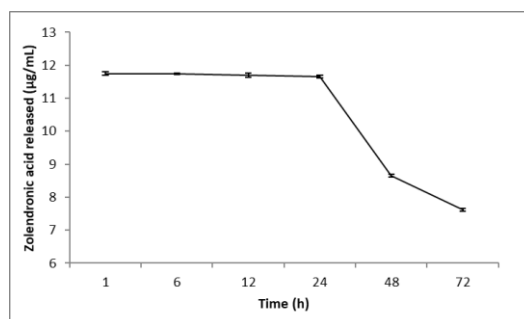


Figure 6.

Release profile of zoledronic acid from BioHA:LiP_ZA structures

The release profile demonstrates a biphasic pattern: an initial steady phase followed by a decline, typical for diffusion-controlled drug release systems. The BioHA coating appears effective in moderating the

release, but a gradual reduction over time suggests possible depletion or diffusion limitations. This release behaviour suggests that the BioHA coating on titanium could be suitable for sustained delivery

of ZA, making it potentially beneficial for long-term therapeutic applications such as bone regeneration or implant-related treatments [19, 20]. Further optimisation could focus on extending the sustained release phase for prolonged drug availability.

Cell proliferation and cytotoxicity

Bone marrow-derived hMSCs were grown in direct contact with the tested material surfaces, and cell viability was investigated after 72 h using the MTS assay.

As shown in Figure 7, the number of viable hMSCs varied significantly among the analysed coatings at 72 h post-seeding. Cells adhered to BioHA and BioHA:LiP coatings exhibited lower MTS absorbance values compared to those grown on bare Ti (CTRL Ti), whereas the viability of cells grown on BioHA:LiP_ZA coatings was comparable to that recorded on CTRL Ti. On the contrary, a significant increase in metabolic activity ($p < 0.0001$) was observed for BioHA:LiP_ZA coatings relative to BioHA and BioHA:LiP samples,

suggesting a higher number of viable cells on the biomaterial surface at 72 h post-seeding. This enhancement is likely attributed to the beneficial effect of ZA doping.

To evaluate the potential indirect cytotoxic effects of coatings on hMSC, cells adhered for 24 h were exposed to the conditioned medium obtained from the tested materials after 72 h of incubation, followed by cell viability assessment. In this experimental setup, none of the analysed coatings exhibited cytotoxic effects (Figure 7). Notably, adding ZA to the BioHA:LiP coatings resulted in a statistically significant increase ($p < 0.0001$) in hMSC proliferation upon exposure to the extracted medium, suggesting a favourable influence of ZA on cell growth.

In conclusion, all synthesised structures demonstrated no cytotoxic effects on hMSCs. Furthermore, cell viability tests indicated that incorporating ZA as a doping agent enhanced hMSC proliferation on the coated surfaces.

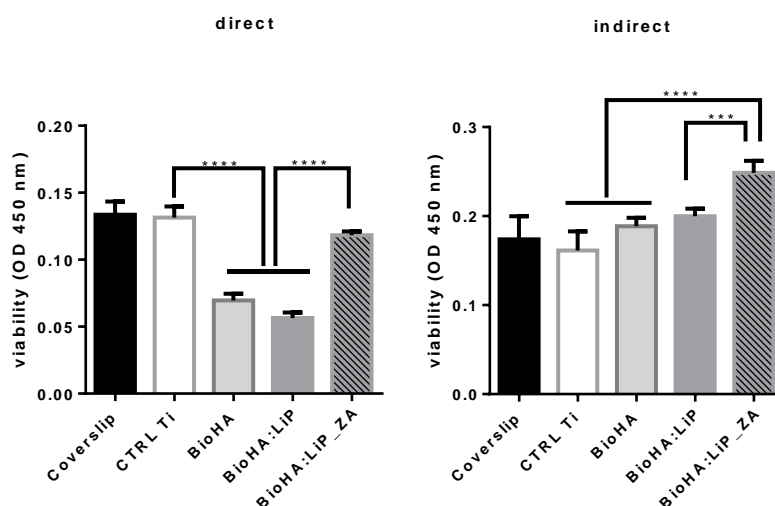


Figure 7.

Viability of hMSC cells after 72 h: (a) in direct contact with the tested surfaces (Coverslip, CTRL-Ti, BioHA, BioHA:LiP, and BioHA:LiP_ZA) in direct contact assays; and (b) upon exposure to the conditioned medium obtained from the incubation of the tested surfaces in indirect contact assays. Results are presented as mean \pm standard deviation from triplicate samples in each group. Statistical significance was determined using two-way ANOVA: *** $p < 0.001$, **** $p < 0.0001$, indicating significant differences between groups

Our findings align with those reported by Misra *et al.*, who demonstrated that ZA enhances hMSC proliferation, reduces DNA damage accumulation, and promotes differentiation toward the osteogenic phenotype [21]. Similarly, Fliefel *et al.* observed that the effect of ZA on hMSC viability and survival is concentration-dependent, with lower ZA concentrations shown to enhance osteogenic differentiation [22].

Cell morphology

Human MSCs serve as a reliable *in vitro* model for evaluating various material coatings in tissue engineering and osseous implantology studies.

In our experiments, hMSCs were labelled with Alexa488-phalloidin to stain actin filaments and assess cell morphology 72 h post-seeding on MAPLE-coated surfaces compared to control samples (Figure 8).

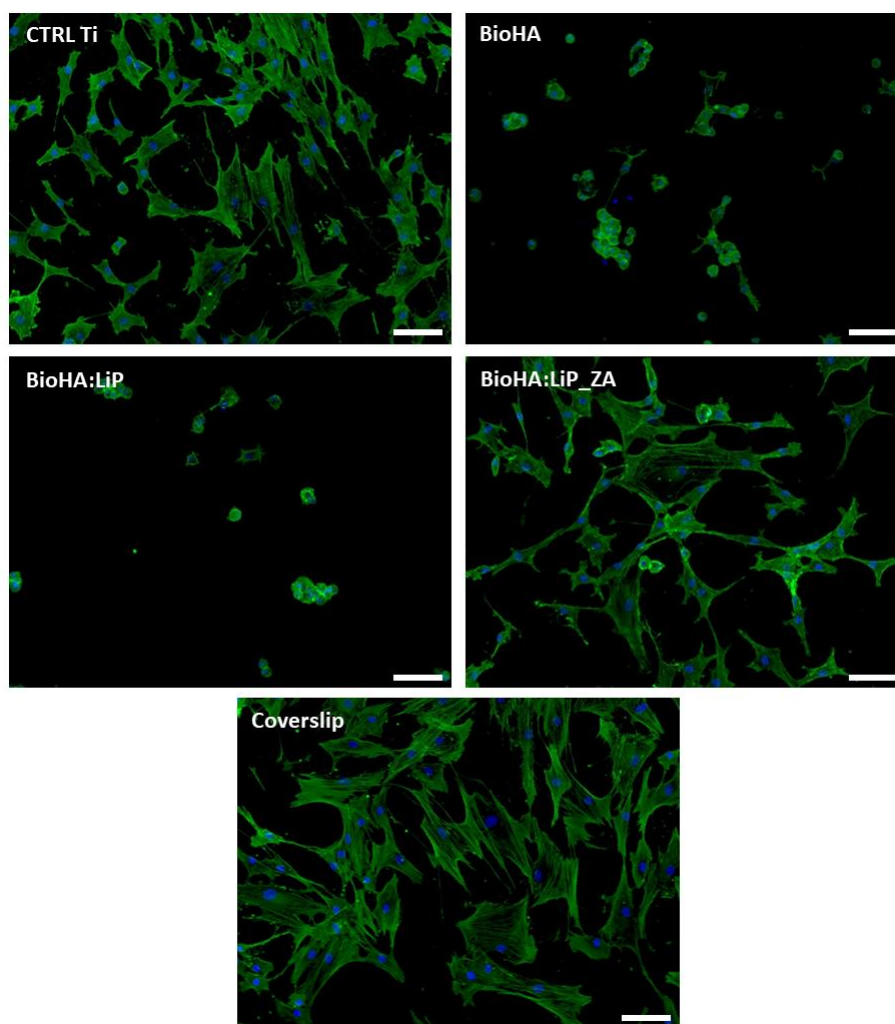


Figure 8.

Fluorescence microscopy images of hMSC cell adhesion and spreading on tested surfaces (Coverslip, CTRL-Ti, BioHA, BioHA:LiP, and BioHA:LiP_ZA) after 72h of culture. Merged images show actin filaments stained with Alexa488-conjugated phalloidin (green) and nuclei counterstained with Hoechst (blue). Images were acquired at 10× magnification, with a scale bar of 100 μm

Human MSCs adhered to unprocessed Ti surfaces (*e.g.*, CTRL Ti) and coverslips, exhibiting typical fibroblast-like morphology characterised by elongated filopodia and well-defined nuclei. Phalloidin staining revealed a well-organized cytoskeleton, with prominent and elongated actin filaments aligned along the major cell axis, suggesting a strong adhesion to the control surfaces (*e.g.*, CTRL Ti and coverslip).

Compared to cells grown on CTRL Ti, hMSCs cultured on both BioHA and BioHA:LiP surfaces exhibited altered morphological features, as observed in fluorescence microscopy images. Predominantly, cells appeared round, individually or in clusters, with reduced adhesion and limited spreading. These findings are consistent with the results of direct viability assays, which indicated impaired cell viability on these surfaces.

In contrast, hMSCs grown on BioHA:LiP_ZA surfaces exhibited elongated filopodia, a branched

morphology, and enhanced spreading, facilitating improved interaction with both neighbouring cells and the coating surface.

It is well known that cell morphology is closely linked to stem cell differentiation. Kumar *et al.* Reported that a branched morphology correlates with hMSC differentiation toward the osteogenic lineage. Specifically, their study demonstrated that a branched, osteocyte-like phenotype can induce osteogenesis of human bone marrow-derived stem cells, even in the absence of osteoinductive factors [23]. Similarly, our findings revealed that a branched morphology of hMSCs observed at 72 h of culture promoted increased osteogenic differentiation in response to lactoferrin-based composite coatings [24].

Conclusions

We report on this study on the fabrication of biological-derived hydroxyapatite doped with lithium phosphate

(BioHA:LiP) coatings (synthesised by pulsed laser deposition) and BioHA:LiP functionalised with zoledronic acid (BioHA:LiP_ZA) bi-layered structures (synthesised by matrix-assisted pulsed laser evaporation technique). The fabricated structures were characterised from the structural, morphological, compositional, and biological points of view.

The comparative FTIR spectra highlighted the structural and chemical modifications induced by the incorporation of ZA. The sharper and more intense phosphate bands in BHA:LiP_ZA as compared to BioHA:LiP sample suggested a higher degree of crystallinity in the first case. This finding was in accordance with XRD results. The observed shift in the Ca/P ratio toward a slightly higher value in BioHA:LiP_ZA structures, compared to BioHA:LiP films, indicated the successful ZA adsorption. *In vitro*, biocompatibility investigations showed a lack of chemically induced cytotoxicity for all tested materials. Additionally, ZA doping was demonstrated to improve the adhesion and spreading of osteogenic progenitor stem cells to the MAPLE-obtained BioHA:LiP coatings. These findings suggest that ZA-functionalized BioHA:LiP coatings exhibit promising properties for implant surface modifications, warranting further investigation for biomedical applications. A potential future direction involves optimising drug encapsulation strategies within BioHA:LiP coatings to achieve controlled and sustained release of ZA. Incorporating biodegradable carriers, such as polymeric (PLGA) or lipid-based nanocapsules, could enhance drug stability, enable tunable release kinetics, and ensure a prolonged therapeutic effect while minimising systemic toxicity.

Acknowledgement

This work was financially supported by the Romanian Ministry of Research, Innovation, and Digitization under Romanian National Nucleu Program LAPLAS VII—Contract no. 30N/2023. PF, MI and LES acknowledge the support of the Romanian Academy Research Programme (2024-2025).

Conflict of interest

The authors declare no conflict of interest.

References

1. Amini AR, Laurencin CT, Nukavarapu SP, Bone tissue engineering: Recent advances and challenges. *Crit Rev Biomed Eng.*, 2012; 40(5): 363-408.
2. Wu Y, Sun B, Tang Y, Shen A, Lin Y, Zhao X, Li J, Monteiro MJ, Gu W, Bone targeted nano-drug and nano-delivery. *Bone Res.*, 2024; 12(1): 51.
3. Li G, Zhang L, Wang L, Yuan G, Dai K, Pei J, Hao Y, Dual modulation of bone formation and resorption with zoledronic acid-loaded biodegradable magnesium alloy implants improves osteoporotic fracture healing: An *in vitro* and *in vivo* study. *Acta Biomater.*, 2018; 65(Suppl 1): 486-500.
4. Jayaram R, O'Donnell PW, Puleo DA, Systems for local, sustained release of zoledronic acid as a potential treatment for metastatic bone disease. *Mater Sci Eng C*, 2021; 118: 111395.
5. Billings C, Anderson DE, Role of implantable drug delivery devices with dual platform capabilities in the prevention and treatment of bacterial osteomyelitis. *Bioengineering*, 2022; 6; 9(2): 65.
6. Zureigat OA, Neamtu J, Duța L, Icriverzi M, Florian P, Sima LE, Dorcioman G, Grumezescu V, Bălăsoiu RM, Buteică SA, Văruț RM, Nicolaescu OE, Development and characterisation of implantable sandwich structures made of lithium-doped biological-derived hydroxyapatite and ciprofloxacin. *Farmacia*, 2024; 72(6): 1415-1426.
7. Duta L, Popescu AC, Current status on pulsed laser deposition of coatings from animal-origin calcium phosphate sources. *Coatings*, 2019; 9(5): 335.
8. Florian PE, Duta L, Grumezescu V, Popescu-Pelin G, Popescu AC, Oktar FN, Evans RW, Roseanu Constantinescu A, Lithium-doped biological-derived hydroxyapatite coatings sustain *in vitro* differentiation of human primary mesenchymal stem cells to osteoblasts. *Coatings*, 2019; 9(12): 781.
9. Bingul MB, Gul M, Dundar S, Bozoglan A, Kirtay M, Ozupek MF, Ozcan EC, Habek O, Tasdemir I, Effects of the Application Local Zoledronic Acid On Different Dental Implants in Rats On Osseointegration. *Drug Des Devel Ther.*, 2024; 18: 2249-2256.
10. Qayoom I, Raina DB, Širka A, Tarasevičius Š, Tägil M, Kumar A, Lidgren L, Anabolic and antiresorptive actions of locally delivered bisphosphonates for bone repair: a review. *Bone Joint Res.*, 2018; 7(10): 548-560.
11. Zhang J, Bai H, Bai M, Wang X, Li Z, Xue H, Wang J, Cui Y, Wang H, Wang Y, Zhou R, Bisphosphonate-incorporated coatings for orthopedic implants functionalization. *Mater Today Bio.*, 2023; 22: 100737.
12. Nie J, Zhang S, Wu P, Liu Y, Su Y, Electrospinning with lyophilized platelet-rich fibrin has the potential to enhance the proliferation and osteogenesis of MC3T3-E1 cells. *Front Bioeng Biotechnol.*, 2020; 8: 595579.
13. Aguilar P, Fonseca AC, Garlet GP, Gulinelli JL, Santos PL, Influence of zoledronic acid and low-intensity laser on collagen fibers during the bone repair process. *Acta Cir Bras.*, 2024; 39: e393724.
14. Reddy LM, Reddy KJ, Reddy PR, A simple RP-HPLC method for related substances of zoledronic acid in pharmaceutical products. *Arab J Chem.*, 2017; 10: S196-204.
15. Negroiu G, Piticescu RM, Chitanu GC, Mihailescu IN, Zdrentu L, Miroiu M, Biocompatibility evaluation of a novel hydroxyapatite-polymer coating for medical implants (*in vitro* tests). *J Mater Sci.*, 2008; 19: 1537-1544.
16. Sima LE, Stan GE, Morosanu CO, Melinescu A, Ianculescu A, Melinte R, Neamtu J, Petrescu SM, Differentiation of mesenchymal stem cells onto highly adherent radio frequency-sputtered carbonated hydroxylapatite thin films. *J Biomed Mater Res A*, 2010; 95(4): 1203-1214.
17. Duta L, Oktar FN, Stan GE, Popescu-Pelin G, Serban N, Luculescu C, Mihailescu IN, Novel doped

- hydroxyapatite thin films obtained by pulsed laser deposition. *Appl Surf Sci.*, 2013; 265: 41-49.
18. Duta L, Mihailescu N, Popescu AC, Luculescu CR, Mihailescu IN, Çetin G, Gunduz OĞ, Oktar FN, Popa AC, Kuncser A, Besleaga C, Comparative physical, chemical and biological assessment of simple and titanium-doped ovine dentine-derived hydroxyapatite coatings fabricated by pulsed laser deposition. *Appl Surf Sci.*, 2017; 413: 129-139.
 19. Son JS, Choi YA, Park EK, Kwon TY, Kim KH, Lee KB, Drug delivery from hydroxyapatite-coated titanium surfaces using biodegradable particle carriers. *J Biomed Mater Res B Appl Biomater.*, 2013; 101(2): 247-257.
 20. Ma X, Gao Y, Zhao D, Zhang W, Zhao W, Wu M, Cui Y, Li Q, Zhang Z, Ma C. Titanium implants and local drug delivery systems become mutual promoters in orthopedic clinics. *Nanomaterials*, 2021; 12(1): 47.
 21. Misra J, Mohanty ST, Madan S, Fernandes JA, Hal Ebetino F, Russell RG, Bellantuono I, Zoledronate Attenuates Accumulation of DNA Damage in Mesenchymal Stem Cells and Protects Their Function. *Stem Cells*, 2016; 34(3): 756-767.
 22. Fliefel R, El Ashwah A, Entekhabi S, Kumbrink J, Ehrenfeld M, Otto SJ, Bifunctional effect of Zoledronic Acid (ZA) on human mesenchymal stem cells (hMSCs) based on the concentration level. *Stomatol Oral Maxillofac Surg.*, 2020; 121(6): 634-641.
 23. Kumar G, Tison CK, Chatterjee K, Pine PS, McDaniel JH, Salit ML, Young MF, Simon Jr CG, The determination of stem cell fate by 3D scaffold structures through the control of cell shape. *Biomaterials*, 2011; 32(35): 9188-9196.
 24. Icriverzi M, Bonciu A, Rusen L, Sima LE, Brajnicov S, Cimpean A, Evans RW, Dinca V, Roseanu A, Human mesenchymal stem cell response to lactoferrin-based composite coatings. *Materials*, 2019; 12(20): 3414.